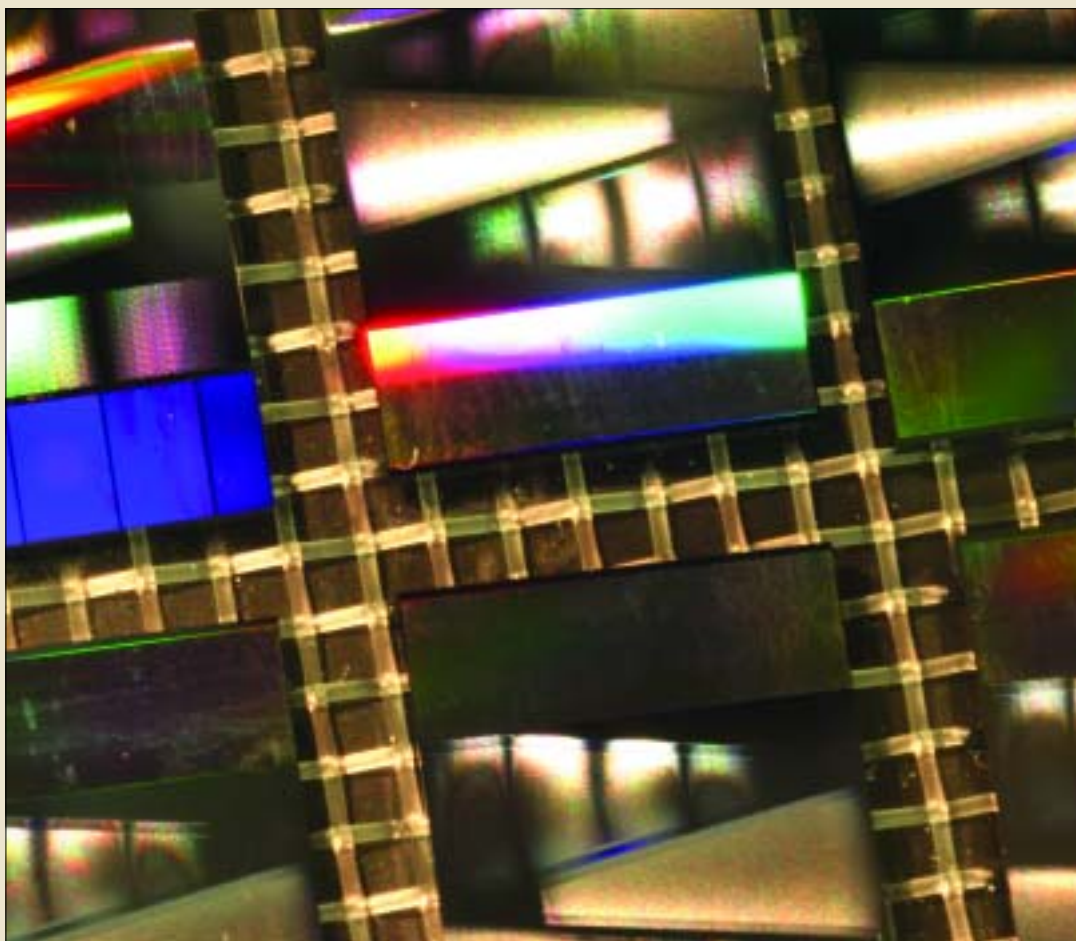


A hand is holding a black rectangular device, likely a photonic integrated circuit. The device has a central area that is illuminated with a bright blue light, showing a complex, layered structure. The text is overlaid on the device.

# Holographic Bragg Reflectors,

## Photonic Bandgaps and Photonic Integrated Circuits

Thomas W. Mossberg, Christoph M. Greiner and Dmitri Iazikov



Significant opportunities can arise abruptly from unexpected discoveries or flow gradually from the integration of a series of evolutionary advances; in the second case, it may be only the perception of opportunity that develops suddenly. In this article we describe an opportunity enabled by a series of developments in materials, guided-wave optics and lithography. It centers on our emerging ability to fabricate centimeter-scale guided-wave photonic structures with nanometer-scale feature size, essentially perfect spatial coherence and entirely arbitrary structure. New applications in photonic transport and processing may emerge when the technique is applied to low index contrast materials in accordance with the basic principles of volume holography and photonic crystals.

---

*(Facing page)* A single holographic Bragg reflector (HBR) die showing channel access waveguides and multiple HBRs. *(Above)* Assortment of HBR die with various test structures.



Testing planar waveguide holographic Bragg reflectors. (*Foreground*) Eight-inch silica-on-silicon wafer inscribed with stepped HBR test structures. The wafer shown has no upper silica cladding. (*Background*) Mounted HBR die under examination.

Over the course of the past few years, a series of fabrication-related developments has created a significant opportunity. It is now possible to produce, at high volume and low cost, devices with essentially arbitrary two-dimensional (2D) spatial patterns: patterns having nanometer-scale pixel size and full spatial coherence over centimeter scales.<sup>1</sup> Such devices can be fabricated through use of deep ultraviolet (DUV) photolithography and laser-written reticles, which are among the standard tools of the electronics industry. In the context of photonics, it is now possible to manufacture slab waveguides that contain essentially perfect volume holographic structures, computer-designed to selectively interact with specific signal beams that provide signal routing and wave-front transformation combined with powerful spectral filtering. In this article, we discuss the fundamentals and applications of computer-designed volume holographic structures<sup>2-5</sup> in slab waveguides. Photonic crystals<sup>6,7</sup> are essentially a subset of such volume holographic structures.

As we will explain, there are fundamental functional advantages to structures and devices that employ low rather than high refractive index contrast. Structures of high index contrast have received substantial attention as enablers of photonic bandgap structures. On the other hand, low index contrast volume holographic structures provide a unique approach to mode-specific signal control. Exploitation of mode-specific signal control in device design can give rise to integrated circuits that are distinctively photonic, in which optical signals freely overlap and intermingle—a situation that cannot be achieved by use of the wire-analog, channel-waveguide-based signal routing architectures currently in vogue. We conclude with a detailed look at a specific holographic device structure, the holographic Bragg reflector,<sup>2</sup> which can be used in multiplexing and spectral filtering.

Historically, volume holograms<sup>8,9</sup> were created through direct exposure of a photosensitive material to multiple writing fields in the context of a precise, interferometric process constrained by the availability of suitable optical fields, by the stability of such fields and by recording material properties such as resolution. Thanks to recently developed fabrication tools, arbitrary planar holograms can be lithographically fabricated on the basis of computer-generated patterns without the need for laser writing beams of complex spatial character. Additionally, silica and other waveguide materials of current interest comprise an extraordinarily stable and robust substrate. The general function provided by a volume hologram is to transform signal beams that match a simulated design input beam into a beam closely matching a simulated design output beam. The transformation may include spectral filtering and wave-front reshaping. Signal routing may include interaction with multiple volume holograms in succession.

Photonic crystals are materials the dielectric structure of which can be described in terms of a lattice of equivalent points and a structure basis that is positioned at each lattice point, in analogy with the crystals of solid-state physics. Photonic crystals exhibit a high degree of translational and angular symmetry. Much attention has been directed to the fabrication of photonic

crystals that exhibit photonic bandgaps, i.e., spectral regions in which the crystal does not support propagating field modes. Bandgaps were originally conceived of as a means of controlling spontaneous radiative emission rates and properties<sup>10</sup>; in that regard, they have profound significance.<sup>11, 12</sup> As may be apparent from the discussion below, however, it is not at all clear whether photonic bandgaps or variations on them provide optimal signal handling solutions.

There is a close relationship between holograms and photonic crystals. In fact, photonic crystals might be described as the subset of volume holograms that can be produced via the interference of two or more plane wave optical fields. The Fourier transform of a 2D photonic crystal provides a plane wave decomposition of the structure. Since interference of plane waves from that decomposition will reproduce the crystal, the crystal structure can be considered a volume hologram. Unlike photonic crystals, which by definition are translationally invariant, holograms may comprise structures outside the narrow range of translationally invariant crystalline possibilities. For example, simulated interference of optical beams that diverge or converge to the access ports of an integrated photonic circuit can be captured in a holographic structure and used to control such signals.

Optical devices typically require high net reflectivity. High reflectivity can be produced via the interaction of many spatially extended weak scatterers (extended scattering) or via interaction with a few spatially localized strong scatterers (localized scattering). Extended scattering allows for the use of low refractive index contrast structures that exhibit low polarization sensitivity and low loss. Extended scattering also introduces a high degree of wave-front specificity to the scattering process. In the case of simple plane wave scattering, this leads to the Bragg condition. In the case of non-plane-wave fields, it leads to wave-front-selective scattering.<sup>9</sup>

Interestingly enough, mode-selectivity, which is desirable in the context of mode-specific signal control in integrated photonic circuits, is fundamentally incompatible with the existence of full, delocalized, photonic bandgaps. The reason is illustrated in Fig. 1. In Figs. 1(a)-1(d), two crystal-type spatial refractive index distributions (left) and their 2D Fourier transforms are shown. The transforms reveal those plane wave modes that can cooperatively scatter from the medium without multiple scattering. They provide useful insight into how scattering strength (index contrast) correlates with mode-selectivity. Figure 1(a) is configured to represent a crystal-type extended scattering medium with a scattering length (roughly the distance light penetrates into the scattering medium before reflection) of about 10 lattice spacings. Its transform, shown in Fig. 1(b), indicates that only plane wave modes with narrow ranges of  $k$ -vector amplitude and direction are cooperatively scattered. Figure 1(c) models a crystal-type localized scattering medium, the scattering length of which is on the order of one lattice spacing (very strong interfacial scattering). Examination of the transform of this system shows that plane wave modes over significantly larger ranges of angles and spatial frequencies are scattered. One has the signature of a photonic bandgap when

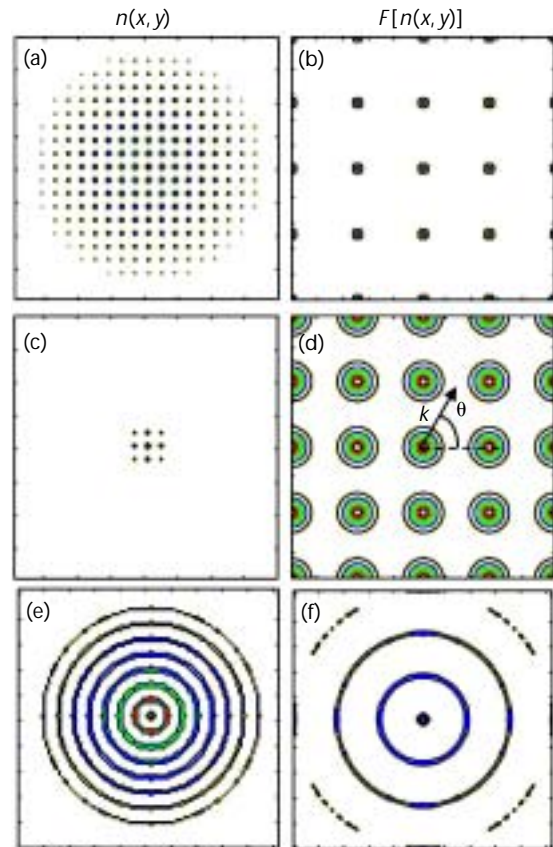


**Figure 1.** (Left) Three different spatial refractive index profiles representing scattering environments as seen by centrally located observers. (Right) 2D Fourier transforms of the refractive index distributions. The index profile of (e) does not have crystal-type translational invariance and displays a spatially localized bandgap.

scattering ranges overlap, providing for isotropic scattering of modes throughout a band of spatial frequencies. For scattering ranges to overlap, a material must have a very short scattering length; this implies very strong single-interface scattering, which in turn implies high refractive index contrast. This conclusion, which follows from basic Fourier principles, is only weakly dependent on structural factors such as lattice and basis type. Note also that the structures of Figs. 1(a) and 1(c) are space filling, which provides for a translationally invariant scattering picture.

In Figs. 1(e) and 1(f), we consider an extended system with holographic-type spatial order (interference between converging and diverging cylindrical waves). Because the spatial order shown is not translationally invariant, the environment and resultant scattering picture will look different to observers located in various locations. Figure 1(e) represents the environment as seen by an observer located at the center of the holographic structure. The refractive index distribution shown in Fig. 1(e) exhibits extended scattering, with a scattering length of about 10 spatial periods. Its transform, shown in Fig. 1(f), is very different from that of Fig. 1(b), in that broad angular

ranges of plane wave modes are strongly scattered despite the extended nature of the scattering interaction. A “spatially localized” photonic bandgap is present at the center of the circular structure. The existence of this local bandgap does not require strong scatterers. As the scatterers get weaker, making the scattering length larger, the width of the localized bandgap gets narrower but the bandgap itself does not disappear.

It has been suggested that crystal-type materials can be employed to construct integrated channel waveguides with sharp bends and to implement other useful functions in integrated optical circuits.<sup>6, 7</sup> To force all exposed optical signals to follow desired pathways by blocking all alternatives, these functions generally employ a strongly scattering bandgap material. Signal handling via holographic-type materials proceeds according to an opposite principle. Holographic structures designed with extended weak scatterers couple exclusively to targeted signal modes, routing them from point-to-point within an integrated photonic circuit which provides in-route wave-front shaping and spectral filtering while remaining inert to other signal beams that are simultaneously being controlled by other collocated, dedicated holographic structures. One can imagine an engineered holographic transport fabric with unconfined optical signals freely flowing from source to destination with all signals mutually impervious to one another. Signals may propagate freely only to be tightly focused (localized) at their destination. Beam matching to disparate ports and active devices in the integrated circuit falls within the available holographic wave-front shaping function. Holographic signal transport fabrics enable powerful new architectures for integrated photonic circuits combining localized and delocalized signal flow, free signal overlap and in-route spectral selectivity.

Although there has long been awareness of the basic principles that enable holographic signal transport fabrics, their application in photonic integrated circuits has been blocked until recently by our inability to produce them. Today, however, the situation has changed dramatically: for the most part, we can assert that if it can be designed, it can be built. The opportunities that result are substantial.

As an example, a simple holographic signal control structure—a holographic Bragg reflector (HBR)—is depicted in Fig. 2. In this example the structure, which is implemented in a 2D slab waveguide, comprises contours etched on the top of the core waveguide layer. The inset at right depicts a cross section of the device showing diffractive contours etched into the core layer and filled with cladding material. For single-mode silica devices operating in the 1.5- $\mu\text{m}$  region, the waveguide core can be 2-5  $\mu\text{m}$  thick and the cladding layers can be 10-20  $\mu\text{m}$  thick. The HBR shown acts as a focusing reflector with a structure-programmed spectral transfer function.

The HBR input signal's spatial wave front is determined by the detailed properties of the input port. The contours of the HBR optimally comprise computer-generated holographic elements capable of transforming the input wave front into a back-propagating mode, the spatial wave front of which is matched for entry to the output port. While it is tempting to view the process in terms of simple ray based imaging and point sources,

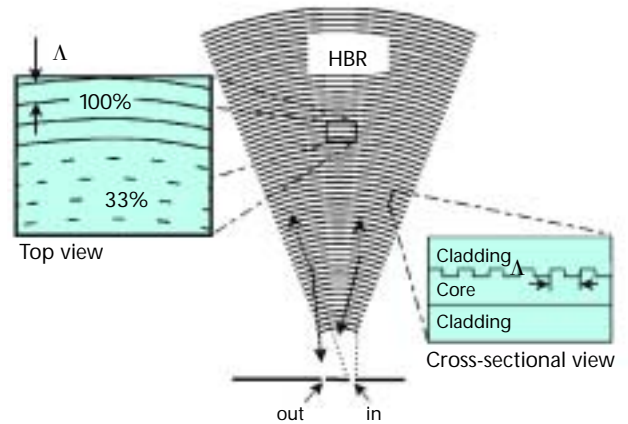


Figure 2. Simple two-port holographic Bragg reflector.

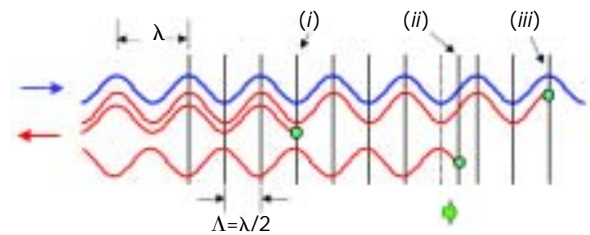


Figure 3. Schematic of a 1D Bragg reflector showing in-phase and phase-shifted reflection. The top sine wave represents the right-going input field. The next two sine waves represent in-phase reflections from regularly positioned scattering surfaces. The bottom sine wave shows a phase-shifted reflection produced by a displaced scatterer. Continuous phase control follows from continuous scatterer displacement.

the achievement of optimal signal throughput requires consideration of the real signal wave fronts as well as the determination of contour profiles that provide optimal matching. Diffractive contours, such as circular arcs or ellipses, can be used, provided that their well known imaging aberrations do not have a critical impact on performance. The average spacing between contours is set to about half the in-medium optical wavelength of light to be backscattered. The detailed spacing between contours may be varied to achieve phase-based apodization (see Fig. 3).

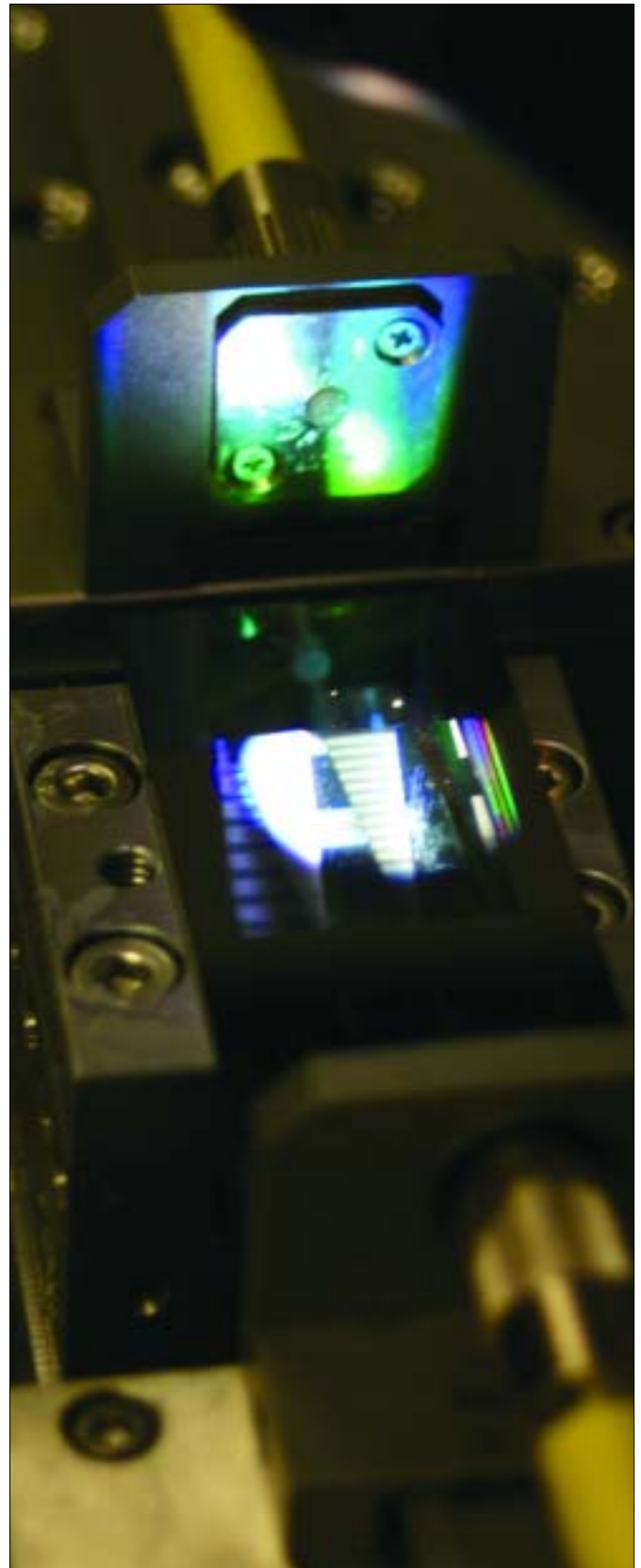
The HBR shown in Fig. 2 is configured as a first order device. As emerges from diffraction theory, such devices can also be designed using higher diffractive orders. The advantages of higher order devices include their consistency with lower resolution lithographic means and, in the case of even diffraction orders, their ability to direct light out of the waveguide

plane along a surface normal. Disadvantages include loss of light to the various out-of-plane diffraction orders and lower diffractive coupling strength per unit length for the same waveguide geometry. Structures such as the HBR shown in Fig. 2 can be fabricated with 0.25- $\mu\text{m}$ -resolution DUV reduction photolithography, where a laser-written reticle is imaged with demagnification onto a photoresist-coated substrate. Since spatial coherence is very important in HBRs, the materials and tools used in fabricating them must provide full spatial coherence over length scales important in a particular design. Critical material and tool issues include the ability of the laser writer to produce a true model of the computer-generated HBR design, the ability of the photolithographic tool to accurately project the reticle onto the device substrate and the effective refractive index uniformity within the slab waveguide, which in turn is controlled by the uniformity of waveguide materials and dimensions. It has been demonstrated that HBRs produced with standard production-grade photolithographic tools can exhibit full spatial coherence over centimeter scales.<sup>1</sup> Coherence over centimeter scales provides for spectral resolutions at the level of 10 GHz and allows the use of scatterers so weak that 10,000-plus contours must cooperate in order to produce high reflectivity. In 1-cm devices, strong back reflection is produced by refractive index contrast of significantly less than one percent at the contour faces. On the other hand, more compact higher index contrast devices are equally possible.

Diffractive structures in general, and HBRs in particular, are frequency selective. In the limit of low reflectivity, the reflection spectrum of a suitably designed HBR is simply proportional to a 1D spatial Fourier transform of the HBR structure as a function of round trip optical depth into the device.<sup>2</sup> In this respect, an HBR behaves similarly to a fiber Bragg grating—except that the HBR output is directionally distinct. As reflectivity increases, the relationship between HBR structure and spectrum becomes more complex, and theoretical tools such as those already implemented for fiber gratings must be brought to bear in spectral calculations. Nevertheless, it is still true that control of HBR longitudinal structure provides broad spectral programming capability. Fabrication via modern photolithography, which provides full control over the properties of individual diffractive contours, offers unprecedented potential for spectral programming. Key to achieving broad spectral programming capability is a phase and amplitude apodization method that is compatible with available lithographic tools.

In the case of laser-written and photolithographically fabricated devices, phase apodization is quite straightforward. Spatial displacement of contours by a quarter wavelength introduces a phase shift of  $\pi$  (see Fig. 3). Full range, arbitrary, bipolar phase shifts are achieved via judicious contour placement.

Amplitude apodization requires improvisation. The etching process favors the production of devices with diffractive contours of constant depth across a device wafer. For this reason, the obvious approach to amplitude apodization—namely varying contour depth—is challenging. Fortunately, several more subtle, but more lithographically friendly approaches to amplitude apodization are available. The HBR maps a signal wave



HBR die mounted in test jig. Butt-coupled single-mode fibers inject signals and collect spectrally filtered output.

front onto an output wave front via diffraction from contours. The contours are typically long (millimeter scale) compared to available lithographic resolution ( $<1 \mu\text{m}$ ). It follows that the contours can be written as a series of dots or dashes instead of as a continuous trench (see Fig. 2, *left inset*). Analysis shows that the effective diffractive amplitude of a contour can be made to vary in proportion to the fraction of the contour being etched. A suitable level of attention to details, including the pattern of dots or dashes comprising the contour, also leads to preservation of wave-front matching (imaging) properties.<sup>1</sup>

There is a second order effect associated with partial-etch amplitude apodization: the effective refractive index of the slab waveguide varies slightly in proportion to the local spatial density of the trenches. Spectral designs must take into account the correlation of amplitude apodization and effective refractive index. There are alternative amplitude apodization methods available that do not perturb local waveguide index. The apodization methods described depend to a great extent on the powerful contour-by-contour control provided by modern DUV photolithographic fabrication tools.

A given HBR will interact significantly only with optical signals characterized by wavelengths and wave fronts that fall within a certain range. This makes it possible to place multiple HBRs in close proximity on a single slab waveguide device through superposition, interleaving, or simply close spacing (see Fig. 4). Such a configuration allows, for example, for the implementation of spectral multiplexers.<sup>13</sup> In a multiplexer, signals with various wavelengths enter a device through distinct ports and are combined via a wavelength-selective means into a common output port. It is possible to use a group of HBRs to perform this function; in this case, each HBR maps signals from a specific spatial input port to the common output port. Because of the powerful spectral programming capability of photolithographically fabricated HBRs, channel passband functions can be engineered independently in great detail (see Fig. 5).

Devices that use multiple HBRs in close proximity must be designed to be consistent with photolithographic constraints. No problems arise when HBRs are either interleaved or placed in close proximity without actual spatial overlap. But great care must be exercised in the case of direct superposition, or in other words when multiple HBR structures are overlaid on common real estate on the design reticle and on the slab waveguide.

With a binary-etch process, overlaying multiple HBRs will quickly lead to the etching of most of the reticle and hence slab waveguide surface, which in turn will lead to a loss of function. Superposition can, however, be achieved by use of the partial contour writing approach described above. If the contours of each HBR are only partially written, the chance of trench overlap decreases.

By suitable choice of the contour writing fraction and implementation in the design algorithm of overlap avoidance routines, potentially large numbers of HBRs can be directly overwritten. One must keep in mind, however, that by reducing the fraction of contours that are etched, one reduces their net reflectivity.

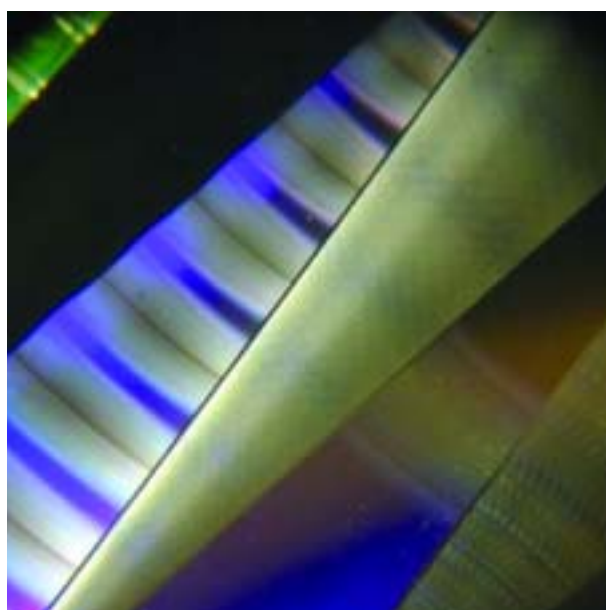
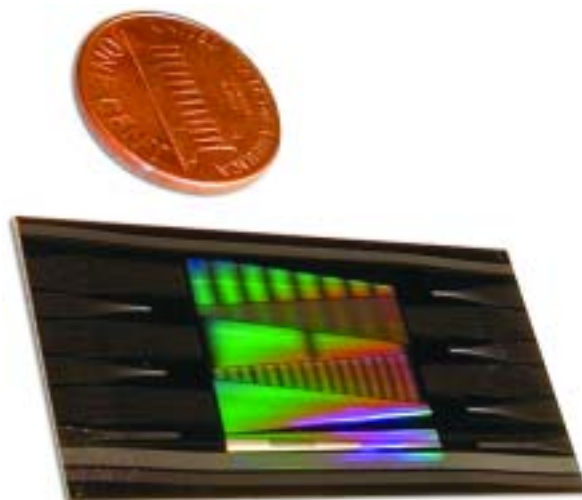


**Figure 4.** Photograph of fabricated holographic Bragg reflectors. Each wedge-shaped object is comprised of multiple interleaved, superimposed or stacked HBRs. Each HBR couples light from one channel-waveguide input to a channel-waveguide output while spectrally filtering it. Channel waveguides are the fine curved lines. To enhance structural visibility, the chips shown have no upper cladding.

Aside from multiplexing and simple signal transport, HBRs can enable a number of other functions in the areas of spectral and temporal signal processing. They can be configured, for example, to form the basis of an integrated spectral comparator,<sup>14</sup> in which input signals of unknown spectra can be simultaneously fed to multiple HBRs, each programmed with a spectral signature (that represents, for example, a chemical compound). By monitoring the relative strength of the HBR outputs, it is possible to closely match the signal spectra to one of the HBR programmed reference spectra. It is especially excit-

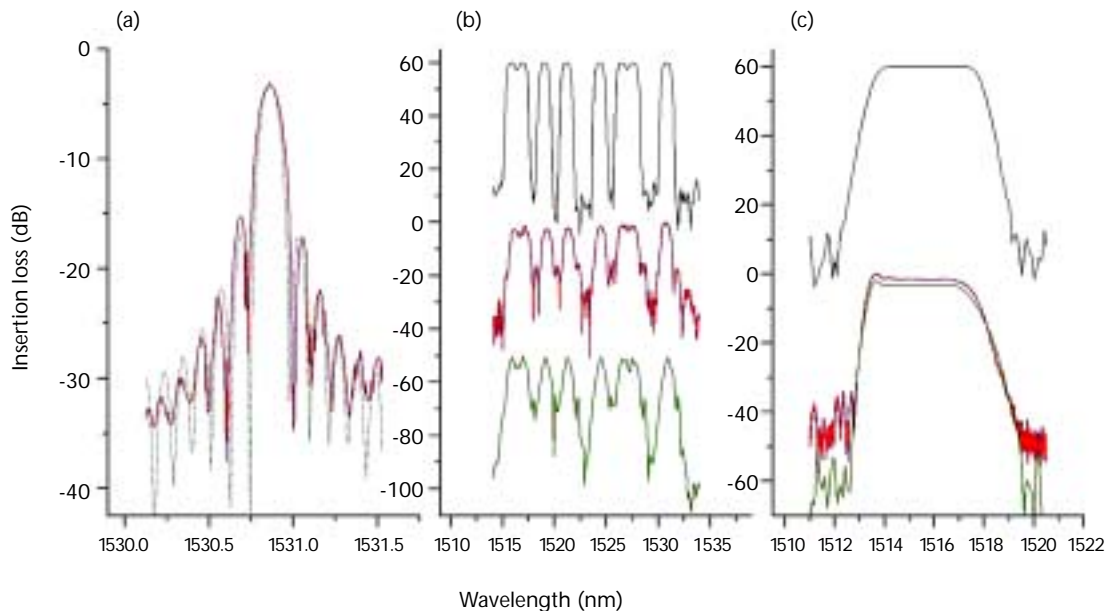


**Figure 5.** Measured and simulated spectral transfer functions of HBR devices showing various features: (a) high spectral resolution, (b) complex multi-peaked spectrum, (c) flat-top wide bandwidth. The green lines are simulations including amplitude-apodization-induced variations in effective refractive index (see text). The red lines are measured spectral transfer functions. The black lines are original design simulations that neglect coupling between amplitude apodization and effective refractive index. Excellent agreement between full simulation and measured spectra indicates powerful spectral programmability.


ing to note that by use of existing lithographical technologies and standard silica-based materials, centimeter-scale HBRs can be engineered to produce strong reflection over bandwidths spanning hundreds of nanometers with spectral feature resolution as low as 10 GHz—a truly high performance filter.

In summary, we have discussed the interaction of optical signals with spatially ordered materials having crystal-type or holographic-type spatial order. We have described how holographically ordered structures such as HBRs provide powerful signal-mode-specific functionality, including spectral filtering and wave-front transformation. Spatially extended HBR structures are largely transparent to non-targeted optical modes and fully consistent with fabrication friendly, low loss and largely polarization insensitive, low-refractive-index-contrast materials. Use of HBRs to provide signal routing and processing may lead to uniquely new and powerful integrated optical circuits, enabled through the combination of the holographic concept and modern photolithographic fabrication techniques. This is especially true since fabrication techniques have finally matured to the point that virtually any holographic design can be implemented. In the longer term, volume holographic waveguide optical devices appear entirely consistent with low cost stamping or nanoprinting based fabrication. All this suggests that HBRs and related devices are poised to make an important

contribution to the future of integrated photonics circuits. They could also redefine our current perceptions of photonics application and integration possibilities.

### Acknowledgments

We would like to thank B. Brainard, Z. Dong, N. Gopinathan, D. Nakamoto, S. Thekdi and A. Vaidyanathan for fabrication magic.

 Thomas W. Mossberg (twmoss@LightSmyth.com), Christoph M. Greiner and Dmitri Iazikov are with LightSmyth Technologies Inc., Eugene, Ore.

### References

1. C. Greiner et al., *J. Lightwave Tech.* **22**, 136 (2004).
2. T. W. Mossberg, *Opt. Lett.* **26**, 414 (2001).
3. G. Tricoles, *Appl. Opt.* **26**, 4351 (1987).
4. S. Reinhorn et al., *Appl. Opt.* **37**, 3031 (1998).
5. W. Yu et al., *Appl. Opt.* **41**, 96 (2002).
6. D. W. Prather, *Opt. Photon. News* **13**(6), 16-9 (2002).
7. A. Scherer et al., *IEEE Trans. Nanotechnol.* **1**(1), 4-11 (2002).
8. R. K. Kostuk et al., *Appl. Opt.* **25**, 4362 (1986).
9. J. Shamir and K. Wagner, *Appl. Opt.* **41**, 6773 (2002).
10. E. Yablonovitch, *Phys. Rev. Lett.* **58**, 2059 (1987).
11. S. John and T. Quang, *Phys. Rev. A* **50**, 1764 (1994).
12. T. W. Mossberg and M. Lewenstein, *J. Opt. Soc. Am. B* **10**, 340 (1993).
13. D. Iazikov et al., "Apodizable integrated filters for coarse WDM and FTTH-type applications," accepted for publication in *J. Lightwave Tech.* (May 2004).
14. T. W. Mossberg et al., "Planar-waveguide integrated spectral comparator," *J. Opt. Soc. Am. A.* (6/1/04 issue).